frontiers | Frontiers in Materials

TYPE Original Research
PUBLISHED 26 June 2023
DOI 10.3389/fmats.2023.1196156

OPEN ACCESS

EDITED BY
Marco Alfano,
University of Waterloo, Canada

REVIEWED BY
Giangiacomo Minak,
University of Bologna, Italy
Muhammad Umair,
National Textile University, Pakistan
Kadir Bilisik,
Erciyes University, Türkiye

*CORRESPONDENCE
Xin Zhang,
zhangx8@sustech.edu.cn
Dan Yang,
danyang@cczu.edu.cn

RECEIVED 29 March 2023
ACCEPTED 13 June 2023
PUBLISHED 26 June 2023

CITATION
Miao Y, Ni J, Zhu K, Liu Y, Chang Y, Gong Z, Yang D and Zhang X (2023), Effect of aramid core-spun yarn on impact resistance of aramid/epoxy composite.
Front. Mater. 10:1196156.
doi: 10.3389/fmats.2023.1196156

Effect of aramid core-spun yarn on impact resistance of aramid/epoxy composite

Yajing Miao[1], Jiahuan Ni[2,3,4], Kai Zhu[2,3], Yizhou Liu[2,3], Yu Chang[2,3], Zixin Gong[2,3], Dan Yang[2,3]* and Xin Zhang[1]*

[1]Department of Mechanics and Aerospace Engineering, Southern University of Science and Technology, Shenzhen, China, [2]School of Materials Science and Engineering, Changzhou University, Changzhou, China, [3]National Experimental Demonstration Center for Materials Science and Engineering, Changzhou University, Changzhou, China, [4]Hua Lookeng Honors College, Changzhou University, Changzhou, China

Introduction: The surface of aramid filament is smooth, which is a great defect for impact resistance and composite molding of aramid/epoxy composite. In this study, a new type of yarn—aramid core-spun yarn is introduced to the fabrication of compositematerials. It increases the friction among yarns and optimizes the performance of yarns.

Methods: To verify the improvement of yarn in the composite material, the hand lay-up process is used, and the first layer and the fourth layer are replaced by core-spun yarns in a four-layer composite configuration.

Results and Discussion: The energy absorption, and the damage of the impacted surface and the back surface are evaluated through the drop weight impact test. The yarn pull-out test can reflect the internal friction of fabric. The results show that the average energy absorption of new yarn in the first layer is 10 J cm^2/g more than that in the fourth layer at a 90°/45°/-45°/0° configuration after the normalization, but the conclusion is contrary when the structure is -45°/0°/90°/45°. Under the structure of 90°/45°/-45°/0°, the damaged area of the fabric is larger when the aramid core-spun yarn is laid on the first layer, while a contrary result can be found for the structure of -45°/0°/90°/45°. The fundamental research will provide design ideas and supports for aramid composite.

KEYWORDS

core-spun yarn, energy absorption, composite materials, damage mechanism, impact resistance

1 Introduction

With the rapid development of science and technology, the research and use of high-performance materials (Ali et al., 2019; Mahesh et al., 2021a; Harussani et al., 2022) are becoming increasingly popular. Optimization of various materials for improving impact resistance is very common (Wang et al., 2015; Zhang X. et al., 2018; Li et al., 2023). The aramid fiber is used as bulletproof material and is very common to the public due to its high strength and high modulus, which makes it superior to soft body armor. However, the aramid fiber is characterized by a smooth surface, the interface between the layers is easy to be debonded, and the friction between them is relatively small. When the fabric is impacted, the layers of fabric will be delaminated. Meanwhile, the friction between the fabric and drop hammer is also small, leading to weakened resistance and lower energy absorption capacity.

Researchers have taken many ways to improve the friction properties of the aramid fiber. First, from a microscopic aspect, sodium ionization and graft modification on the surface of the aramid fiber have been carried out (Zhang QP. et al., 2018); Sheng et al. (2020) applied ultrasonic impregnation technology to modify the aramid fiber, which is environmentally friendly and convenient for industrial production. Aramid nanofibers (ANFs) were added to the matrix, for example, Li T. et al. (2021) impregnated aramid and carbon fabric with the ANF solution by the dipping coating method. After the modification, the roughness and polarity of the fibers were significantly improved. Meanwhile, the shear strength of laminates, I-mode fracture toughness (G_{IC}), and bending properties of composites were also significantly improved; Bilisik et al. (2018) and Bilisik et al. (2019) improved the interlayer shear strength of the composite by the short beam method; improving the friction performance between yarns by ZnO (zinc oxide) nanowire coating (Nasser et al., 2020), applying shear thickening fluid (Li et al., 2019; Yeh et al., 2019; Qin et al., 2020; Mahesh et al., 2022) to the surface of the aramid fabric, and increasing its impact resistance by non-Newtonian fluid are other ways. Second, from a macroscopic aspect, the adjustment of the structure of the aramid fabric (Ralph et al., 2020; Toksoy et al., 2020), stacking mode and the ratio between layers (Ahmad and Bajpai, 2018; Azam et al., 2020), the type of resin used in preparing composite materials, the adhesion degree with the aramid fiber (Wang et al., 2016), thickness of coating (Mahesh et al., 2021b), processing technology (Stopforth and Adali, 2019), density of yarns (Verma et al., 2021), structure (Aryal et al., 2020; Mawkhlieng and Majumdar, 2020; Chatterjee et al., 2021), etc., can be considered. Furthermore, in a complementary way (Mousavi and Khoramishad, 2020), the aramid fiber and other yarns (carbon fiber, date palm fiber, flax, etc.) are woven together (Haro et al., 2018), and a better mechanical property is achieved by adjusting the mixing ratio of the fabric. Meanwhile, the factors of external conditions like temperature also significantly influence the mechanical property of composites (Uzay et al., 2017; Bazli et al., 2019; Jafari et al., 2019; Mhanna et al., 2020; Sharma et al., 2021).

As mentioned previously, there are many ways to change the friction properties of yarns from external conditions, which are key factors that influence the overall mechanical properties of the composite. However, the research on novel yarn for impact resistance has not been studied sufficiently (Wang, 2020; Li YW. et al., 2021; Miao et al., 2021; Sun, 2021). A new type of aramid core-spun yarn, which is an aramid filament wrapped by staple aramid yarn, where staple aramid yarn is a yarn spun from short fibers, is introduced in this study. It can not only enhance the roughness of the yarn but also enhance its elasticity. The interaction between yarns has a significant influence on the impact strength and energy absorption capacity of laminates, so the pull-out test (Bilisik and Korkmaz, 2010; Bilisik, 2011; Bilisik and Korkmaz, 2011) was carried out to measure the bonding force between the pulled yarn and the adjacent yarn. In order to observe the damage degree of the novel yarn after being impacted, the novel yarn is laid on the top layer and bottom layer of the multidirectional aramid/epoxy composite material, respectively. The damage mode of laminates is also very complicated, which affects the impact resistance and energy absorption. Shabani et al. (2023) observed the damage sequence and detailed the damage characteristics of laminates through the verification of finite element simulation. Because of the importance of the damage mode, many researchers have created methods to detect damage (Chen et al., 2022; Fotouhi et al., 2023; Wei and Chen, 2023). The stacking sequence of the selected structure is 90°/45°/-45°/0°, which has better absorbing energy capacity, according to a previous work (Miao et al., 2022). At the same time, the −45°/0°/90°/45° sequence is used as an auxiliary function to verify the change in the absorbing energy after adding the novel yarn. The damage morphology of fabrics on the front and back surfaces after impact is observed accordingly. For the aramid core-spun yarn placed in different layers, we explore which one can absorb more energy. The results of the experiments can provide a reference for the anti-impact field and some ideas for the design of composite structures.

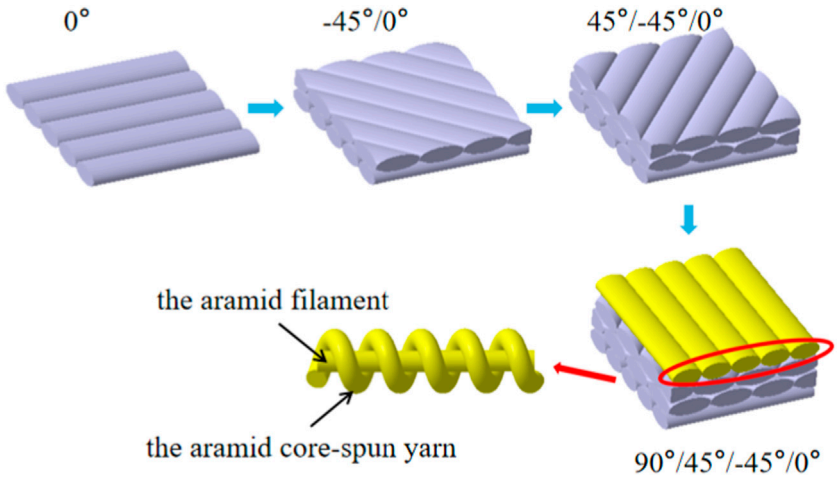

FIGURE 1
Lamination process of composite materials.

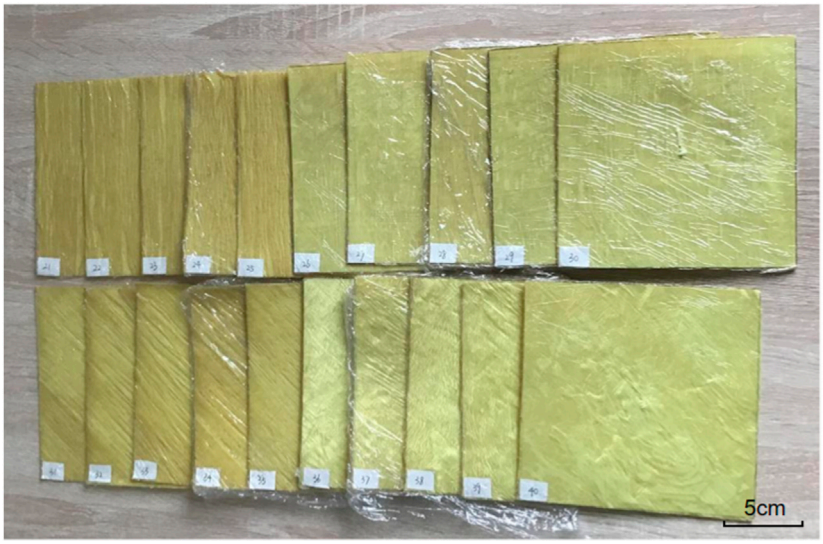

FIGURE 2
Composite materials.

TABLE 1 Specifications of materials.

Material	Linear density (dtex)	Size (mm)	Specimen	Configuration
First layer: aramid core-spun yarn; other layers: Kevlar 129	Kevlar 129: 1,580	150 × 150	A1	90°/45°/-45°/0°
Fourth layer: aramid core-spun yarn; other layers: Kevlar 129	Aramid core-spun yarn: 694		A2	90°/45°/-45°/0°
First layer: aramid core-spun yarn; other layers: Kevlar 129			B1	−45°/0°/90°/45°
Fourth layer: aramid core-spun yarn; other layers: Kevlar 129			B2	−45°/0°/90°/45°

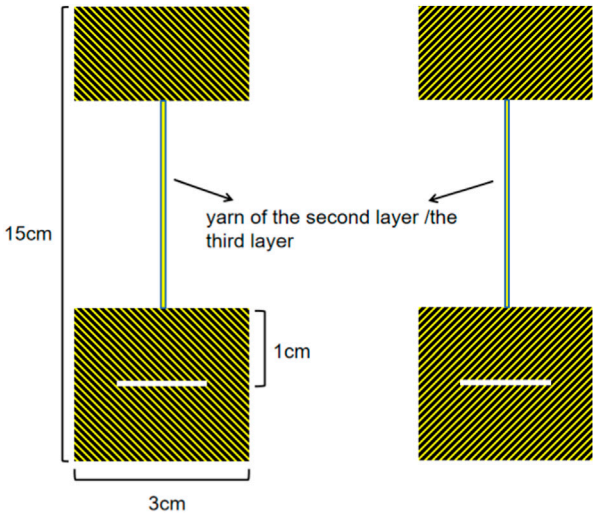

FIGURE 3
Preparation of the sample of the yarn pull-out test.

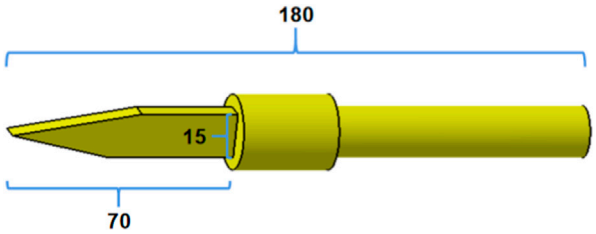

FIGURE 4
Diagram of the knife blade.

2 Experiment and method

2.1 Materials

A composite laminate is made of the aramid yarn and epoxy resin in this study. The aramid yarn is used as reinforcement, and the epoxy resin is used as the matrix. There are two kinds of yarns: Kevlar 129 and the aramid

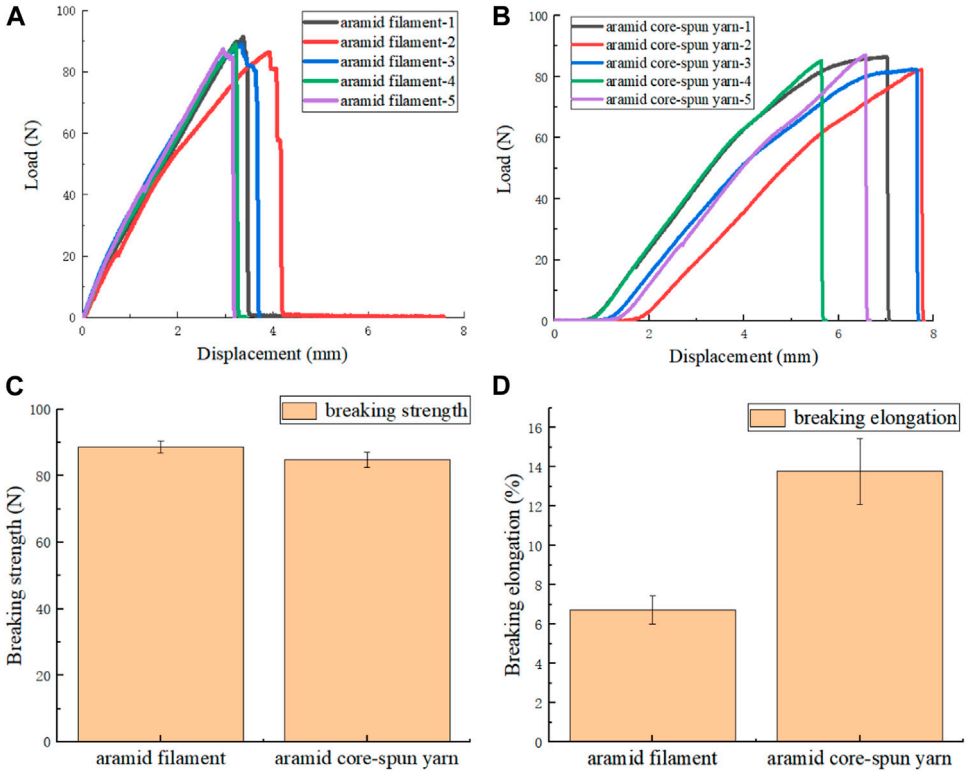

FIGURE 5
Results of the tensile test: **(A)** load–displacement curve of the aramid filament; **(B)** load–displacement curve of the aramid core-spun yarn; **(C)** breaking strength of the aramid filament and aramid core-spun yarn; and **(D)** elongation at the break of the aramid filament and aramid core-spun yarn.

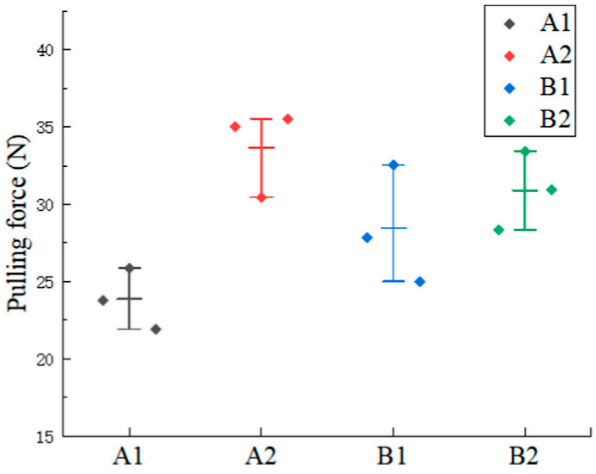

FIGURE 6
Comparison of the peak force of the yarn pull-out experiment.

core-spun yarn. The linear density of Kevlar 129 is 1,580 dtex. A new type of yarn is added to the top or bottom layer of the composite material, and the lamination process of composite materials is shown in Figure 1. The aramid filament is covered with the staple aramid yarn, and the linear density of the aramid core-spun yarn is 694 dtex. The model of the flexible epoxy resin is JEF-0211, and the curing agent is JH-0112, and the weight ratio between them is 5: 1. Detailed information is given in Tables 3, 4.

2.2 Preparation of the fabric

Each layer of yarn is coated with resin using a brush. After reaching four layers, the upper and lower surfaces are covered with a plastic wrap, and the laminate is pressed using heavy objects. It is placed in the oven for 20 min, the temperature is set to 60°C, and then it is air-dried at room temperature again, thus completing the stable molding process of the laminate. Two structures are compared, and the arrangement direction of the yarn is 90°/45°/-45°/0° and −45°/0°/90°/45°. The failure damage mechanism of the impacted surface and back surface is different. So the aramid core-spun yarn is replaced in the first layer and the fourth layer of the two structures, and energy absorption will be different. As shown in Figure 1, it is the process of the first layer of the aramid core-spun yarn with 90°/45°/-45°/0°. Figure 2 shows the laminates.

The laminate with the 90°/45°/-45°/0° structure is marked as A, and the laminate with the −45°/0°/90°/45° structure is marked as B. "1" means that the first layer is replaced with the aramid core-spun yarn, and "2" means that the fourth layer is replaced with the aramid core-spun yarn. The code of the laminate is a combination of letters and numbers. The dimensions of the drop hammer impact test are 150 mm × 150 mm. The specifications of the materials are shown in Table 1.

TABLE 2 Results of the drop hammer impact test.

Sample	Average absorbed energy (J)	Standard deviation	Areal density (g/cm^2)	Average energy absorption after normalization (J·cm^2/g)
A1	4.37	0.10	0.071	61.55
A2	4.82	0.08	0.093	51.83
B1	4.44	0.06	0.089	49.89
B2	4.79	0.06	0.093	51.51

TABLE 3 Technical parameter of the epoxy resin.

Type	Epoxy value (mol/100 g)	Organochlorine (mol/100 g)	Inorganic chlorine (mol/100 g)	Viscosity (mpa/s 25°C)	Gardner
JEF-0211	4.37	0.10	0.071	61.55	≤1

TABLE 4 Technical parameter of the curing agent.

Type	Outward appearance	Amine value (mg KOH/g)	Active hydrogen equivalent	Viscosity (mpa/s 25°C)	Reference amount (phr)	Gelation time (50 g) 25°C	Surface drying time of the thin layer 25°C	Curing system
JH-0112	Colorless to light yellow transparent liquid	450–550	70–75	200–800	35–40	0.4–0.6 h	3–4	Room temperature 24 h

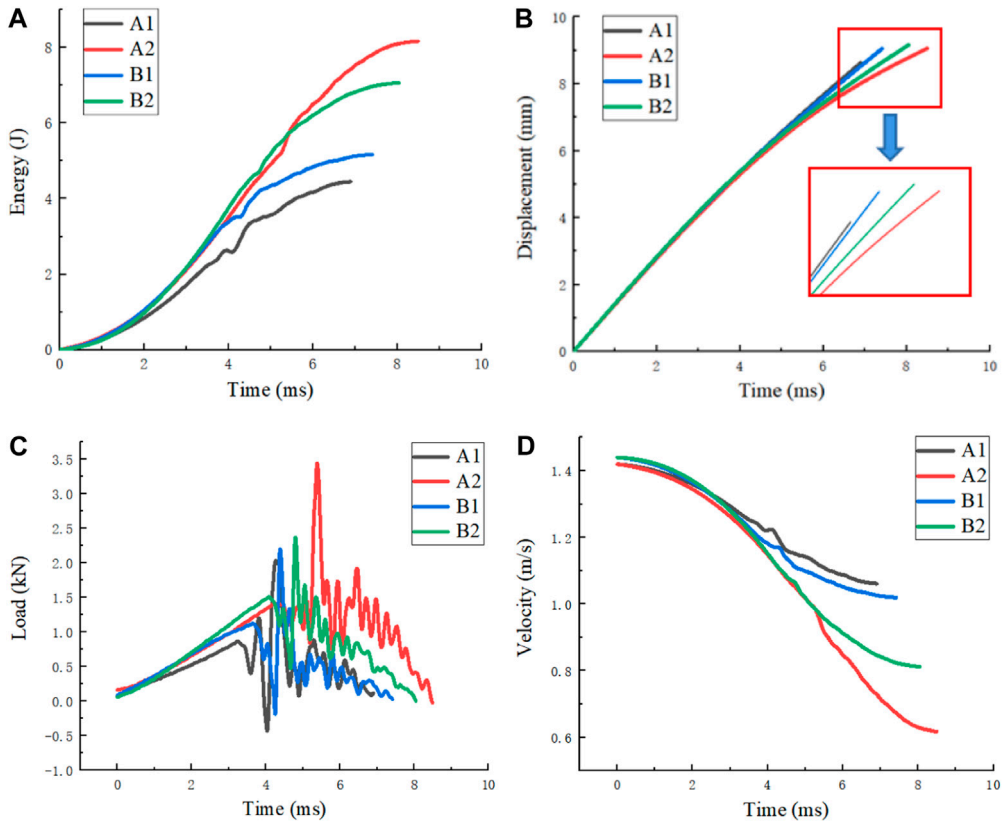

FIGURE 7
(A) Time–energy curve of the impact test; **(B)** time–displacement curve of the impact test; **(C)** time–load curve of the impact test; and **(D)** time–velocity curve of the impact test.

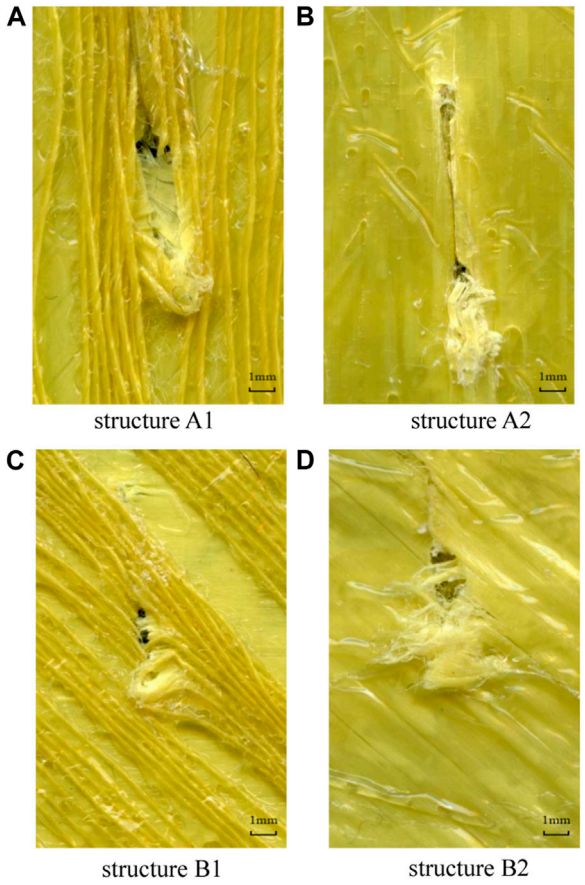

FIGURE 8
Impacted surface under an optical microscope: **(A)** structure A1; **(B)** structure A2; **(C)** structure B1; and **(D)** structure B2.

2.3 Tensile test

The setting method is the strength of a single yarn, the standard is GB/T3916, and the tensile test of yarn is carried out using an electronic fabric strength machine. The clamping distance of each yarn is 50 mm, and the speed is 20 mm/min. Five samples are considered a group; the 625D aramid core-spun yarn is formed by covering a 400D aramid filament with 400D staple aramid yarn, so it is compared with a 400D aramid filament to verify the performance of the novel yarn. The tensile strength of the aramid core-spun yarn is obtained. It is important to observe not only the improvement of the surface friction of the yarn but also the little reduction of the breaking strength of the yarn.

2.4 Yarn pull-out test

The yarn pull-out test is similar to the principle of yarn pull-out when the fabric is impacted. It is meaningful to carry out the test because yarn pull-out is one of the damages formed of the fabric after being impacted. According to GB/T3923.1—2013, the YG(B)026E electronic fabric strength machine is used for the experiment. The speed is set to 100 mm/min, and the size of the sample is 150 mm × 30 mm. Three samples are taken as a group. In order to observe the friction and peak force of the yarn of the fabric inside after adding the aramid core-spun yarn, the yarns pulled out from each group of samples are the adjacent layers closest to the aramid core-spun yarn. Figure 3 shows the preparation of the sample of the yarn pull-out test. As the yarn is vertical during pull-out, the angles of other layers will change relatively.

2.5 Drop weight impact test

The composite material will absorb energy by deformation or damage failure after the drop weight impact test. Because the four layers of multidirectional yarns are bonded with epoxy resin as a whole, the main macroscopic damage is the impacted surface and the back surface of the fabric. The middle layer plays a transitional role, so the first and fourth layers are the main observation objects. In order to study the impact resistance of the two structures, the uppermost layer and the lowermost layer are replaced with the aramid core-spun yarn. A different yarn is used according to a possibility given by the ASTM D3763; the shape of the blade is not the default one, and the impactor is a knife blade. Figure 4 shows the knife blade. During every impact, the direction of the impactor remains the same. The orientation of the blade, with respect to the laminate, is vertically downward. The blade forms 0° with the direction of the first-layer yarn of structures A1 and A2 and 135° with the direction of the first-layer yarn of structures A3 and A4; the size of the sample is 150 mm × 150 mm. Five samples are taken as a group. The part of the conical bayonet connected to the hammer body is 10 kg. The impact energy is set at 10 J. The experimental instrument is the DIT 302E machine.

3 Results and discussion

3.1 Tensile properties

The surface modification of yarn is very important. Increasing the surface friction of the yarn is helpful for energy absorption and fabric formation, but increasing the friction may affect other properties, such as tensile fracture. After the laminate is impacted, the elongation at the break is one of the main damage factors, and it is also the deformation damage of the energy absorption mechanism, so it is necessary to discuss the elongation at the break of a single yarn. In order to study the properties of the aramid core-spun yarn, the single-yarn tensile test is used to test its yarn strength and elongation at break. The aramid filament is taken as a reference to discuss and compare the properties of the aramid core-spun yarn.

As can be seen from Figures 5A, B they are load-displacement curves of the aramid filament and the aramid core-spun respectively. The test is repeated five times, and the average breaking strength of the aramid filament is is 88.663 N. From Figure 5C, the average breaking strength of the aramid core-spun yarn is 84.802 N, which is 4.35% lower than that of the aramid filament. The elongation at the break of the aramid filament is 3.360 mm and that of the aramid core-spun yarn is 6.889 mm, which is 105.03% higher than that of the aramid filament. Figure 5D shows that the elongation at the break of the aramid core-spun yarn is twice more than that of the aramid filament. Although the strength of the core-spun yarn is slightly weakened, its decrease is not obvious. When the fabric is

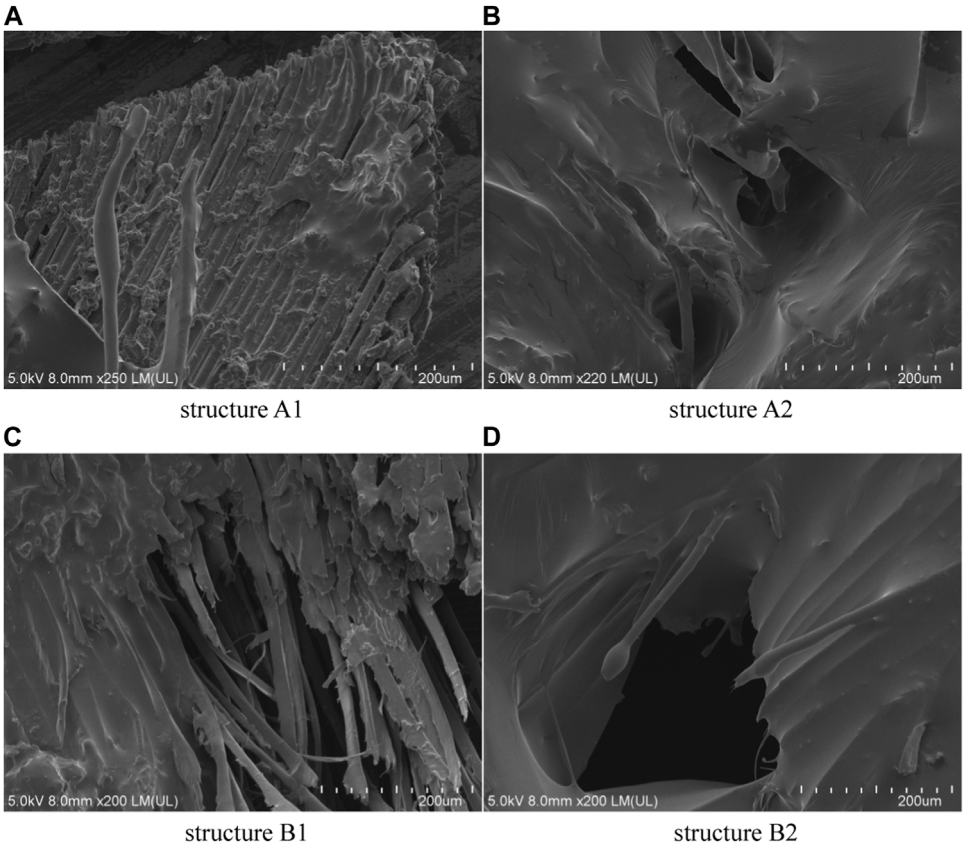

FIGURE 9
Impacted surface under a scanning electron microscope: **(A)** structure A1; **(B)** structure A2; **(C)** structure B1; and **(D)** structure B2.

impacted, the elongation, deformation, and fracture of the yarn are important failure mechanisms, and the increase in the surface friction of the yarn also enhances the energy absorption of the fabric, which can resist the impact more effectively. So, the elongation at the break of the core-spun yarn is greatly improved, which is a great advantage for impact-resistant materials.

3.2 Friction of the internal interface of the fabric

There are many failure behaviors of the impacted composite yarns, and the pull-out of the yarns is one of them. In order to better explore the friction of the aramid core-spun yarn under impact, the yarn pull-out test is carried out on four kinds of samples. Because the stacking sequence of the aramid core-spun yarns also changes, the second and third layers of yarns adjacent to the novel yarns are pulled out.

The results of the three repeated samples are relatively concentrated, and the fluctuation is small. The maximum, minimum, and average values of the four samples are given in Figure 6, and the overall trend is consistent with the trend of the average value. As the structure of A is 90°/45°/-45°/0° and the structure of B is –45°/0°/90°/45°, the numbers "1" and "2" represent the aramid core-spun yarn in the first and fourth layers, respectively, and the pull-out method is carried out on the yarn close to the aramid core-spun yarn. It can be found that in the two structures, the pull-out force of the aramid core-spun yarn in the fourth layer is generally greater than that in the first layer. It may be due to the different overlapping angles or overlapping orders of the intersection points of the aramid filament and aramid core-spun yarn.

If we only consider the phenomenon of the pull-out experiment, the effect of the aramid core-spun yarn laying on the fourth layer will be relatively good. However, the fabric failure caused by the impact is not limited to yarn pull-out, so the yarn pull-out experiment is a reference for the overall energy absorption. The pull-out experiment expounds the failure mechanism of the yarn pull-out after the impact and further refines its damage.

3.3 Energy absorption of the fabric

There are many failure mechanisms of composite materials, including delamination, shearing, crushing, fracture, crack, and deformation. Resin and yarn play an interactive role, and the main energy absorption can be obtained by the drop hammer impact test. The results of laminates prepared using the hand-paste molding process have certain dispersion due to the tests being completed in one batch under the same conditions. As shown in Table 2, there are five samples of each specification. Since the standard deviation is small, indicating

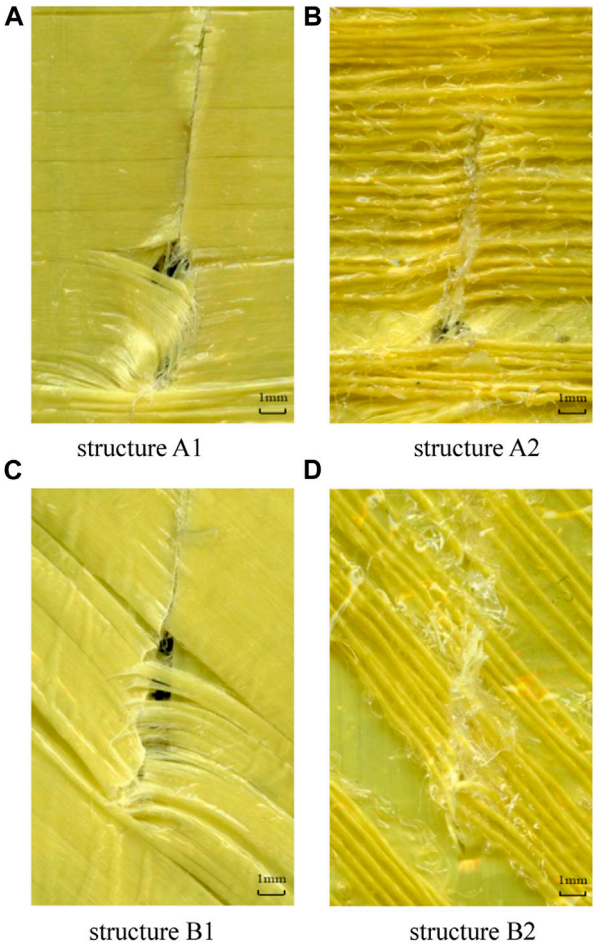

FIGURE 10
Back side under an optical microscope: **(A)** structure A1; **(B)** structure A2; **(C)** structure B1; and **(D)** structure B2.

that the data are stable, the average value is adopted to represent each sample. After unified normalization, the data are corrected and the average value of energy absorption is compared.

From the results of energy absorption, it can be found that the aramid core-spun yarn in the first layer absorbs more energy in structure A, but the result is opposite in structure B. This result is related to the drop direction of the impactor. Because the impactor is conical, the impact on the fabric will not spread evenly, and finally, a crack is formed instead of a round hole. For structure A, the cracks formed are parallel to the first-layer yarns, which means that the angle between them is 0°. This situation is more beneficial to the transmission of impact stress waves. Moreover, the first layer of A1 is covered with aramid core-spun yarns, which further reflects its excellent impact resistance, accelerates the transmission of transverse waves, and makes the energy spread faster and the fabric absorb more. For structure B, the angle between the crack and the direction of the first layer yarn is 45°. Although the first layer is replaced by the aramid core-spun yarn, it does not play its full role, and the lateral diffusion of the stress wave is hindered. On the contrary, the novel yarn replaced at the bottom absorbs more energy. The energy is transferred from the first layer to the last layer, and the longitudinal wave is the same, but the novel yarn at the bottom plays an extreme role, which leads to the opposite result of A and B.

According to kinematics, the velocity $v(t)$, displacement $x(t)$, and applied energy $E(t)$ can be determined according to the contact force $F(t)$. g represents the acceleration of gravity, m represents the mass of the impactor, and v_0 represents the velocity before the impactor collides with the sample.

$$v(t) = v_0 + gt - \int_0^t \frac{F(t)}{m} dt, \tag{1}$$

$$x(t) = v_0 t + \frac{gt^2}{2} - \int_0^t \left(\int_0^t \frac{F(t)}{m} dt \right) dt, \tag{2}$$

$$E(t) = \frac{m\left(v_0^2 - v(t)^2\right)}{2} + mgx(t). \tag{3}$$

As shown in Figure 7, taking time as the abscissa, the impact of four kinds of composite materials is observed. The link between time and energy, time and displacement, time and impact force, and time and velocity is discussed. The overall trends of the four curves of the four composites are similar, which proves the reliability of the results. With the increase in time, A2 and B2 absorb more energy, which is consistent with the yarn pull-out experiment. A1 and B1 absorb more slowly, but this is before the data correction. It is consistent with the data before normalization in Table 2. In the graph of time and displacement, we can observe the smoothness of the line and we can understand that the drop hammer is in free fall. The displacement of A2 and B2 increases slowly in the last stage, which shows that the energy absorption of fabric is higher and the kinetic energy becomes internal energy. By observing the graph of time and force, we know that the peak force of A2 and B2 is higher. The graph of time and speed shows that A2 and B2 make the speed of the impactor decrease rapidly, which shows that kinetic energy is rapidly transformed into the internal energy of the fabric and the fabric will absorb more energy. However, such an overall analysis cannot be separated from the areal density of the fabric, and the later normalization process is also consistent with the figure. So the energy absorption of A1 is higher than that of A2 and that of B2 is higher than that of B1.

3.4 Damage mechanism of the fabric

To explore the damage of different fabrics under impact, we not only analyze the macroscopic morphology but also pay more attention to the microscopic damage mechanism. Considering that the damage situation related to the impact surface and the back surface of the fabric is different, the aramid core-spun yarn is laid on the front and back surfaces of the two structures, respectively. The damage morphology and various interlayer damage states of the fabric after impact are observed. The failure and internal defects of the material both reflect the energy absorption of the fabric, such as the cracking of the laminate and the separation between the resin and the filament. Shearing stress and normal bending stress may be the leading factors.

3.4.1 Influence of the impacted surface of the fabric

As shown in Figure 8, from the observation of the impacted surface, the cross section of structure A1 is rougher than that of

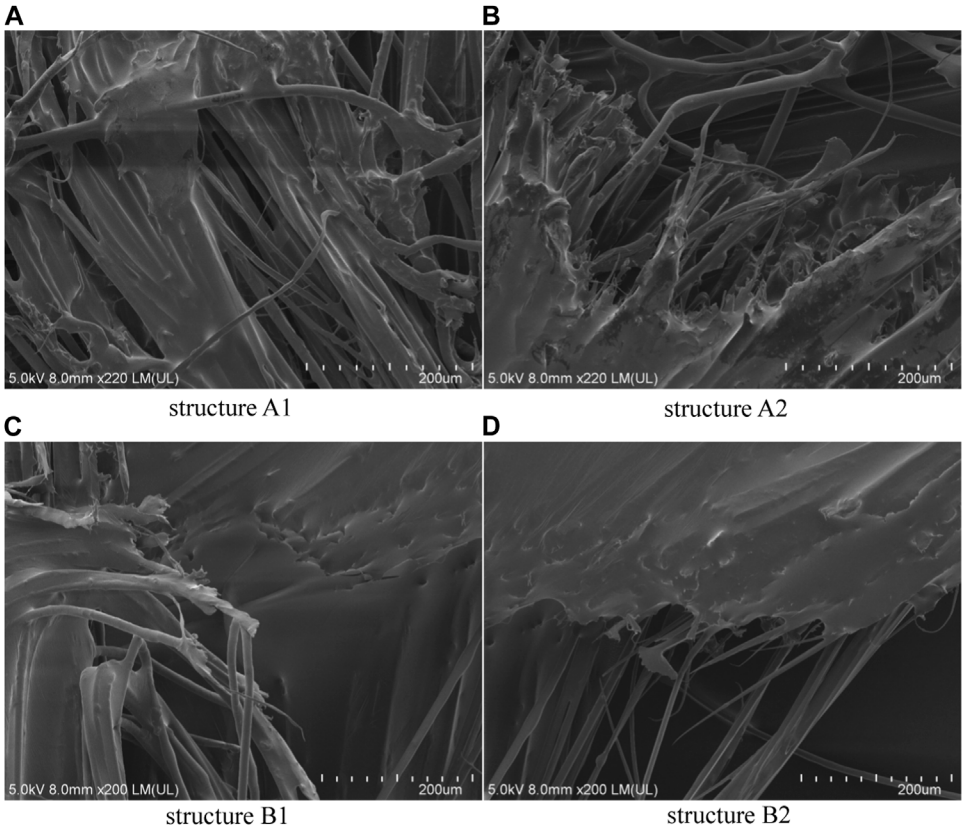

FIGURE 11
Back side under a scanning electron microscope: **(A)** structure A1; **(B)** structure A2; **(C)** structure B1; and **(D)** structure B2.

structure A2, and macroscopically, the damage is more serious. As a layer of the aramid core-spun yarn is laid on the impacted surface of A1, the direction of the bayonet is consistent with the laying direction of the novel yarn, which can transmit stress waves more quickly, and some aramid yarns are pulled out of the fabric surface. On the other hand, the knife edge of the impacted surface of A2 is relatively precise, and some aramid fibers are brought out of the fabric surface, but it is obvious that fibers in the middle of the fabric are brought to the surface. The damaged shapes of the impacted surfaces of structures B1 and B2 are very similar. It can be observed that part of the yarns is cut, and the fiber pull-out area of B2 is larger. The damage of the fiber indicates that the energy absorption will be more, which will also hinder the crack propagation. It can be judged that the toughness and impact resistance of the composite material are better. However, the aramid core-spun yarn on the impacted surface of B1 does not give full play to its own advantages, and the damage is relatively small.

Microscopic analysis is carried out on the damaged parts of the impacted surface. As shown in Figure 9, there are tiny particles near the broken yarn of structure A1, which can be judged as resin breakage, while the absorption of impact energy is partly consumed by resin breakage. The broken yarns of structure A2 are wrapped with resin, and more of them are broken yarns with smooth cuts, and the fiber bundles are not snagged. The yarn fracture of structure B1 is multi-layered, and the fracture of the fiber bundle is uneven, forming a cutting surface of an oblique triangle. The resin distribution is higher on the untwisted yarn. The fiber bundles around the crack of structure B2 are separated due to the impact, and each fiber is coated with a small amount of resin. With the pull-out of some fibers, a part of the resin around is also broken.

3.4.2 Influence of the back of the fabric

The back surface shows that the damage mechanism of the fabrics of four specifications is mainly yarn breakage. As shown in Figure 10, some aramid fibers of structure A1 and structure B1 undergo stretching–breaking–pulling, and the cracks of these fibers are not precise. The remaining part of the crack is clear, and it is directly cut off without stretching. There is a small amount of fiber on the back cut surface of structure A2, which may not reach the force of direct cutting, but it is not stretched, and it is in the middle stage; the pull-out of some fibers also plays a certain role. There are obvious resin cracks on the B2 structure, and the inclination of the angle leads to the cracking of the matrix, which is easily affected by stress.

Through microscopic observation, the damage of the back surface of the composite material is further explored. As shown in Figure 11, the yarns of structure A1 are bonded by resin. There are more resins in some parts; less resin-coated yarns are easier to be cut or stretched, and a small number of pull-out fibers are interlaced among them. The overall crack of structure A2 is relatively flat, but

under the microscope, it can be observed that more fibers are pulled out and stretched, and the fiber and resin are mainly broken together at the damaged part. The fracture between layers is also different. The fibers at the fracture of structure B1 are scattered by the impact, and the damage of the resin is not obvious. The notch of structure B2 shows that the layer-to-layer adhesion is good, and there is no significant delamination. Some fibers are pulled out, and the content of resin on the surface of the pull-out bundles is less. Some fibers of the yarn may be pulled out.

The modification of yarns can improve the impact resistance of composites. By *in situ* ZnO nanorod (Z-NR) grafting (Arora et al., 2020), no matter how the structure of the UHMWPE fabric changes, the increase in friction between the yarns will not change, and the energy absorption and peak force will be greatly improved. In this paper, the aramid core-spun yarn is used to increase the yarn surface roughness, and four types are used to compare the energy absorption, which plays a direct and indirect role during energy absorption and improves the friction performance. Zhou et al. (2016) found that increasing the friction between the projectile and the material is beneficial to the absorption of strain energy and kinetic energy of the material, and increasing the friction between the yarns is beneficial to prevent the yarn from slipping and expanding the area of energy absorption. Duan et al. (2006) found that the decrease in the yarn transverse movement allowed the projectile to load and break more yarns, and the delay in yarn breaking greatly increased the energy absorption of the fabric in the later stage of impact. In the same way, this study is characterized by the aramid core-spun yarn, which increases the surface friction of the aramid fiber and greatly improves the overall energy absorption of the fabric. Under the two structures, the stacking sequence of the aramid core-spun yarn is also an important factor affecting the energy absorption of the fabric.

4 Conclusion

The aim is to study the influence of the aramid core-spun yarn on the impact resistance of composite materials. Two structures of 90°/45°/-45°/0° and −45°/0°/90°/45° are chosen, and the impacted surface and back of composite materials are replaced by the aramid core-spun yarn so as to better observe the impact damage and energy absorption. From the point of view of a single yarn, although the breaking strength of the aramid core-spun yarn is 4.35% smaller than that of the aramid filament, it has advantages in breaking elongation, which is 105.03% higher than that of the aramid filament. When maintaining the strength of the yarn itself, it also increases the elasticity, which improves the toughness of the composite and reduces brittle damage.

The yarn pull-out experiment reflects the friction of the aramid core-spun yarn under impact when it is in two structures and obtains the curve of force and time. It is known that the pulling force of the aramid core-spun yarn in the fourth layer is generally higher than that in the first layer, which is related to factors such as the overlapping angle of intersection point. Yarn pull-out is one of the fracture modes of composite materials after impact, specifically due to the energy absorption of the drop hammer impact. After the correction of normalized energy absorption, structure A1 absorbs approximately 10 J cm^2/g more energy than A2, and B2 absorbs approximately 2 J cm^2/g more energy than B1. The results of the two structures are opposite. So structure A still has better impact resistance and more energy absorption than structure B on the whole.

According to the analysis of the damage mechanism of composite materials by morphology, it can be observed that the damage of structures A1 and A2 is similar and that of structures B1 and B2 is similar. However, A1 is more serious than A2 and B2 is more serious than B1. The damage forms include the cracking of laminate, the separation between the resin and fiber, the breakage of yarn, and the breakage of resin. It shows that the damage mechanism is related to the structure, while the damaged area is related to the stacking sequence of the aramid core-spun yarn and energy absorption. Data analyses have laid a foundation for the follow-up application of the aramid core-spun yarn, opened up the development space for the aramid yarn, and brought more thoughts and inspiration for future research.

Data availability statement

The original contributions presented in the study are included in the article/Supplementary Material; further inquiries can be directed to the corresponding authors.

Author contributions

XZ and DY conceived the research topic and edited the manuscript. YM wrote the first draft of the editorial. JN, KZ, YL, YC, and ZG read and provided significant inputs into all drafts of the editorial. All authors contributed to the article and approved the submitted version.

Funding

This research was supported by the School Start-up Fund Project of Changzhou University (grant number: ZMF21020365) and the 4th Leading Innovative Talents Cultivation Project of Changzhou City (grant number: CQ20210106).

Conflict of interest

The authors declare that the research was conducted in the absence of any commercial or financial relationships that could be construed as a potential conflict of interest.

Publisher's note

References

Ahmad, F., and Bajpai, P. K. (2018). Evaluation of stiffness in a cellulose fiber reinforced epoxy laminates for structural applications: Experimental and finite element analysis. *Def. Technol.* 14 (4), 278–286. doi:10.1016/j.dt.2018.05.006

Ali, A., Adawiyah, R., Rassiah, K., Ng, W. K., Arifin, F., Othman, F., et al. (2019). Ballistic impact properties of woven bamboo-woven E-glass-unsaturated polyester hybrid composites. *Def. Technol.* 15 (3), 282–294. doi:10.1016/j.dt.2018.09.001

Arora, S., Majumdar, A., and Butola, B. S. (2020). Deciphering the structure-induced impact response of ZnO nanorod grafted UHMWPE woven fabrics. *Thin-Walled Struct.* 156, 106991. doi:10.1016/j.tws.2020.106991

Aryal, B., Morozov, E. V., and Shankar, K. (2020). Effects of ballistic impact damage on mechanical behaviour of composite honeycomb sandwich panels. *J. Sandw. Struct. Mater.* 23, 2064–2085. doi:10.1177/1099636220909743

Azam, Z., Jamshaid, H., Nawab, Y., Mishra, R., Muller, M., Choteborsky, R., et al. (2020). Influence of inlay yarn type and stacking sequence on mechanical performance of knitted uni-directional thermoplastic composite prepregs. *J. Industrial Text.* 51, 4973S–5008S. doi:10.1177/1528083720947727

Bazli, M., Ashrafi, H., Jafari, A., Zhao, X-L., Gholipour, H., and Oskouei, A. V. (2019). Effect of thickness and reinforcement configuration on flexural and impact behaviour of GFRP laminates after exposure to elevated temperatures. *Compos. Part B-Engineering* 157, 76–99. doi:10.1016/j.compositesb.2018.08.054

Bilisik, K., Erdogan, G., and Sapanci, E. (2018). In-plane response of para-aramid/phenolic nanostitched and nanoprepreg 3D composites under tensile loading. *Polym. Compos.* 40, 1275–1286. doi:10.1002/pc.24847

Bilisik, K., Gülhan, E. G., and Sapanc, E. (2019). Interlaminar shear properties of nanostitched/nanoprepreg aramid/phenolic composites by short beam method. *J. Compos. Mater.* 53 (21), 2941–2957. doi:10.1177/0021998318811523

Bilisik, K., and Korkmaz, M. (2010). Multilayered and multidirectionally-stitched aramid woven fabric structures: Experimental characterization of ballistic performance by considering the yarn pull-out test. *Text. Res. J.* 80 (16), 1697–1720. doi:10.1177/0040517510365954

Bilisik, K., and Korkmaz, M. (2011). Single and multiple yarn pull-outs on aramid woven fabric structures. *Text. Res. J.* 81 (8), 847–864. doi:10.1177/0040517510391703

Bilisik, K. (2011). Properties of yarn pull-out in para-aramid fabric structure and analysis by statistical model. *Compos. Part A Appl. Sci. Manuf.* 42 (12), 1930–1942. doi:10.1016/j.compositesa.2011.08.018

Chatterjee, V. A., Verma, S. K., Bhattacharjee, D., Biswas, I., and Neogi, S. (2021). Manufacturing of dilatant fluid embodied Kevlar-Glass-hybrid-3D-fabric sandwich composite panels for the enhancement of ballistic impact resistance. *Chem. Eng. J.* 406, 127102. doi:10.1016/j.cej.2020.127102

Chen, Z., Xu, G., Lu, W., Li, C., and Lu, C. (2022). Nonlinear lamb wave imaging method for testing Barely Visible Impact Damage of CFRP laminates. *Appl. Acoust.* 192, 108699. doi:10.1016/j.apacoust.2022.108699

Duan, Y., Keefe, M., Bogetti, T. A., Cheeseman, B. A., and Powers, B. (2006). A numerical investigation of the influence of friction on energy absorption by a high-strength fabric subjected to ballistic impact. *Int. J. Impact Eng.* 32 (8), 1299–1312. doi:10.1016/j.ijimpeng.2004.11.005

Fotouhi, S., Jalalvand, M., Wisnom, M. R., and Fotouhi, M. (2023). Smart hybrid composite sensor technology to enhance the detection of low energy impact damage in composite structures. *Compos. Part A Appl. Sci. Manuf.* 172, 107595. doi:10.1016/j.compositesa.2023.107595

Haro, E. E., Szpunar, J. A., and Odeshi, A. G. (2018). Dynamic and ballistic impact behavior of biocomposite armors made of HDPE reinforced with chonta palm wood (Bactris gasipaes) microparticles. *Def. Technol.* 14 (3), 238–249. doi:10.1016/j.dt.2018.03.005

Harussani, M. M., Sapuan, S. M., Nadeem, G., Rafin, T., and Kirubaanand, W. (2022). Recent applications of carbon-based composites in defence industry: A review. *Def. Technol.* 18 (8), 1281–1300. doi:10.1016/j.dt.2022.03.006

Jafari, A., Bazli, M., Ashrafi, H., Oskouei, A. V., Azhari, S., Zhao, X-L., et al. (2019). Effect of fibers configuration and thickness on tensile behavior of GFRP laminates subjected to elevated temperatures. *Constr. Build. Mater.* 202, 189–207. doi:10.1016/j.conbuildmat.2019.01.003

Li, T., Wang, Z., Zhang, H., Hu, Z., and Wang, Y. J. C. I. (2021a). Effect of aramid nanofibers on interfacial properties of high performance fiber reinforced composites. *Compos. Interfaces* 29 (10), 312–326. doi:10.1080/09276440.2021.1942668

Li, T. T., Dai, W., Wu, L., Peng, H. K., Zhang, X., Shiu, B. C., et al. (2019). Effects of STF and fiber characteristics on quasi-static stab resistant properties of shear thickening fluid (STF)-Impregnated UHMWPE/kevlar composite fabrics. *Fibers Polym.* 20 (2), 328–336. doi:10.1007/s12221-019-8446-6

Li, X., Xu, R., Zhang, X., Zhang, H., and Yang, J. (2023). Inner blast response of fiber reinforced aluminum tubes. *Int. J. Impact Eng.* 172, 104416. doi:10.1016/j.ijimpeng.2022.104416

Li, Y. W., Wang, Y. F., Wang, H. Y., Wang, Y. L., and Zhang, Y. (2021b). Study on absorption and quick-drying property of profiled polyester corn-spun yarn fabric. *Cotton Text. Technol.* 49 (5), 29–32. doi:10.3969/j.issn.1001-7415.2021.05.008

Mahesh, V., Harursampath, D., and Mahesh, V. (2022). An experimental study on ballistic impact response of jute reinforced polyethylene glycol and nano silica based shear thickening fluid composite. *Def. Technol.* 18 (3), 401–409. doi:10.1016/j.dt.2021.03.013

Mahesh, V., Joladarashi, S., and Kulkarni, S. M. (2021a). Damage mechanics and energy absorption capabilities of natural fiber reinforced elastomeric based bio composite for sacrificial structural applications. *Def. Technol.* 17 (1), 161–176. doi:10.1016/j.dt.2020.02.013

Mahesh, V., Joladarashi, S., and Kulkarni, S. M. (2021b). Influence of thickness and projectile shape on penetration resistance of the compliant composite. *Def. Technol.* 17 (1), 245–256. doi:10.1016/j.dt.2020.03.006

Mawkhlieng, U., and Majumdar, A. (2020). Designing of hybrid soft body armour using high-performance unidirectional and woven fabrics impregnated with shear thickening fluid. *Compos. Struct.* 253, 112776. doi:10.1016/j.compstruct.2020.112776

Mhanna, H. H., Hawileh, R. A., Abuzaid, W., Naser, M. Z., and Abdalla, J. A. (2020). Experimental investigation and modeling of the thermal effect on the mechanical properties of polyethylene-terephthalate FRP laminates. *J. Mater. Civ. Eng.* 32 (10). doi:10.1061/(asce)mt.1943-5533.0003389

Miao, L. L., Meng, X. Y., Yu, M. Y., Shen, G. J., and Zou, Z. Y. (2021). Development and application progress of elastic core-spun yarn product. *Cotton Text. Technol.* 49 (1), 76–80. doi:10.3969/j.issn.1001-7415.2021.01.020

Miao, Y. J., Liu, S., Zhu, K., Yang, D., Xin, B. J., and Li, J. C. (2022). Effect of yarns in multiple directions on impact resistance of aramid/epoxy composites. *J. Text. Inst.* doi:10.1080/00405000.2022.2131358

Mousavi, M. V., and Khoramishad, H. (2020). Investigation of energy absorption in hybridized fiber-reinforced polymer composites under high-velocity impact loading. *Int. J. Impact Eng.* 146, 103692. doi:10.1016/j.ijimpeng.2020.103692

Nasser, J., Steinke, K., Hwang, H. S., and Sodano, H. (2020). Nanostructured ZnO interphase for carbon fiber reinforced composites with strain rate tailored interfacial strength. *Adv. Mater. Interfaces* 7 (1), 1901544. doi:10.1002/admi.201901544

Qin, J., Guo, B., Zhang, L., Wang, T., Zhang, G., and Shi, X. (2020). Soft armor materials constructed with Kevlar fabric and a novel shear thickening fluid. *Compos. Part B-Engineering* 183, 107686. doi:10.1016/j.compositesb.2019.107686

Ralph, C., Baker, L., Archer, E., and McIlhagger, A. (2020). Optimization of soft armor: The response of single-ply para-aramid and ultra-high molecular weight polyethylene fabrics under ballistic impact. *Text. Res. J.* 90, 1713–1729. doi:10.1177/0040517519900384

Shabani, P., Li, L., Laliberte, J., Qi, G., Rapking, D., and Mollenhauer, D. (2023). High-fidelity simulation of low-velocity impact damage in fiber-reinforced composite laminates using integrated discrete and continuum damage models. *Compos. Struct.* 313, 116910. doi:10.1016/j.compstruct.2023.116910

Sharma, S., Tiwari, S. K., and Shakya, S. (2021). Mechanical properties and thermal conductivity of pristine and functionalized carbon nanotube reinforced metallic glass composites: A molecular dynamics approach. *Def. Technol.* 17 (1), 234–244. doi:10.1016/j.dt.2020.04.004

Sheng, X., Ren, H., Mou, C. Q., and Li, J. X. (2020). Study on the application of aramid fiber surface modification. *China Insp. Body&Laboratory* 28 (1), 21–24. doi:10.16428/j.cnki.cn10-1469/tb.2020.01.006

Stopforth, R., and Adali, S. (2019). Experimental study of bullet-proofing capabilities of Kevlar, of different weights and number of layers, with 9 mm projectiles. *Def. Technol.* 15 (2), 186–192. doi:10.1016/j.dt.2018.08.006

Sun, J. F. (2021). Discussion on the variety classification and production technology factors of core-spun yarn. *Wool Text. J.* 49 (6), 15–20. doi:10.19333/j.mfkj.20200503606

Toksoy, A. K., Arikan, V., Karakuzu, R., Arman, Y., and Goren, A. (2020). Experimental study on spall behavior of single and multi-plate composites behind armor subjected to shaped charge. *J. Compos. Mater.* 54, 3491–3499. doi:10.1177/0021998320916229

Uzay, C., Boztepe, M. H., Bayramoglu, M., and Geren, N. (2017). Effect of post-curing heat treatment on mechanical properties of fiber reinforced polymer (FRP) composites. *Mater. Test.* 59 (4), 366–372. doi:10.3139/120.111001

Verma, K. K., Viswarupachari, C. H., Gaddikeri, K. M., Ramesh, S., Kumar, S., and Bose, S. (2021). Unfolding the effects of tuft density on compression after impact properties in unidirectional carbon/epoxy composite laminates. *Compos. Struct.* 258, 113378. doi:10.1016/j.compstruct.2020.113378

Wang, P., Zhang, X., Zhang, H., Li, X., He, P., Lu, G., et al. (2015). Energy absorption mechanisms of modified double-aluminum layers under low-velocity impact. *Int. J. Appl. Mech.* 7 (6), 1550086. doi:10.1142/s1758825115500866

Wang, S., Zhang, X. F., Jiang, S. Y., and Inc, D. E. P. (2016). short kevlar fiber reinforcement at the interface for repair of concrete. *J. Mater. Civ. Eng.* 28, 738–742. doi:10.1061/(ASCE)MT.1943-5533.0001611

Wang, Y. H. (2020). Analysis on influencing factors of main performance of spandex core spun yarn. *Text. Rep.* 39 (11), 21–22. doi:10.3969/j.issn.1005-6289.2020.11.008

Wei, L., and Chen, J. (2023). An integrated modeling of barely visible impact damage imaging of CFRP laminates using pre-modulated waves and experimental validation. *Compos. Struct.* 304, 116372. doi:10.1016/j.compstruct.2022.116372

Yeh, S. K., Lin, J. J., Zhuang, H. Y., Chen, Y. C., Chang, H. C., Zheng, J. Y., et al. (2019). Light shear thickening fluid (STF)/Kevlar composites with improved ballistic impact strength. *J. Polym. Res.* 26 (6), 155. doi:10.1007/s10965-019-1811-8

Zhang, Q. P., Xiong, Y. Z., Dai, J., and Wang, Q. (2018b). Study on grafting graphene oxide with modified aramid fiber. *J. Synthetic Cryst.* 47 (9), 225–230. doi:10.16553/j.cnki.issn1000-985x.2018.09.035

Zhang, X., Zhang, H., Wang, P., Chen, Q., Li, X., Zhou, Y., et al. (2018a). Optimization of shear thickening fluid encapsulation technique and dynamic response of encapsulated capsules and polymeric composite. *Compos. Sci. Technol.* 170. doi:10.1016/j.compscitech.2018.11.040

Zhou, Y., Zhang, S., Gong, X., and Xu, A. (2016). Research progress on influence of friction on ballistic performance of flexible materials. *J. Text. Res.* 37 (8), 160–164. doi:10.13475/j.fzxb.20150503205